

A topology of grid connected photovoltaic inverter with variable power factor

Andrey Mirev¹, Yovko Rakanov^{2,*}, Juliana Javorova³, and Anton Andonov⁴

^{1, 2, 4} University of Chemical Technology and Metallurgy, Dept. of Electrical Engineering and Electronics, 8 Kliment Ohridski Blvd., 1756 Sofia, Bulgaria

³ University of Chemical Technology and Metallurgy, Dept. of Applied Mechanics, 8 Kliment Ohridski Blvd., 1756 Sofia, Bulgaria

Abstract. By outlying renewable energy sources, the reactive electric power of local consumers at the same area must be carried by the grid. This loads and causes losses in the same grid. This can be avoided if the necessary reactive power is generated on the spot by the inverter. For that purpose is proposed and investigated a new modified topology for operating with variable power factor. Features of this topology are: transformerless connection to single-phase grid, symmetrical operation in both half waves and the presence of flying inductor, which eliminate the necessity from a separate boost converter, if the input voltage is smaller than the grid peak voltage. The simulation analysis is done on the model elaborated on the SIMETRIX software environment. The results show that the suggested topology can operate with variable power factor and has many additional advantages.

1 Introduction

The most photovoltaic (PV) inverters injecting electrical energy from renewable sources into the grid operate with power factor equal to one. [1-3]. In many cases, especially when the outlying consumers obtain part or all their energy from alternative sources, trough the grid flows the necessary reactive power [4-7]. This causes extra losses in the grid [1]. Inverters that can operate with variable power factor can balance the reactive power immediately in the area of the renewable source and reduce the losses in the grid [1].

Many of the “transistor-bridge” type PV-inverters have the ability to operate with variable power factor, because they have the possibility for reversible flow of the energy during a part of each half wave [1, 2, 9]. In that case, the capacitors, applied to the input of the topology must have a sufficient capacitance to absorb the energy portions.

The “transistor bridge” topology has some disadvantages. They create variable potential of the photovoltaics, which leads to current leakages trough parasitic capacitance between the photovoltaic and the metal PV-frame, respectively the ground [8-15]. At high operating frequency of the inverter, these leakages get illegal value. There are many topologies, which block the operating frequency, and only the low grid frequency ones generate current leakages. Therefore, the values of the current leakages are lower and acceptable. Such are the topologies as: HERIC [9, 13], H5 [9, 10], H6 [9, 10] and other.

Most of the so-called “Flying inductor” topologies operate only by power factor equal to one. Such kind of topology is proposed in [10] and investigated in [11]. It

is called “Flying Inductor Symmetric Topology” (FIST) and it is shown in Fig. 1. Additional details about this topology can be found in the above mentioned papers [10, 11].

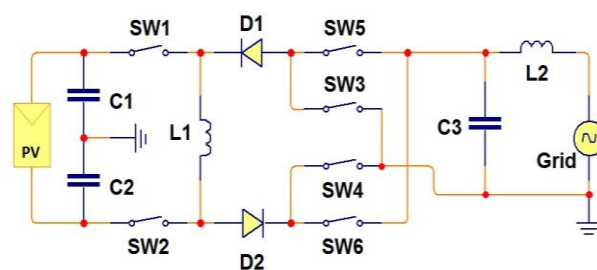


Fig. 1 The Flying Inductor Symmetric Topology “FIST”.

The aim of the current paper is to present a new modified version of the FIST topology from [10, 11], which must be able to operate with variable power factor. It will be carried out simulation, study and analysis of the above mentioned modification of that Flying Inductor Symmetric Topology.

2. Description of the proposed topology

The modifications of the FIST topology are shown with dotted lines on Fig. 2. The free current pathway in the pauses between pulses is changed. The symmetrical operation in both half waves is reserved, and all the advantages as a result also.

Because of the fact that the topology is fully symmetrical to both halves of the current, only the work

* Corresponding author: yovko_rakanov@abv.bg

in the positive half-wave will be considered. At this half-wave, the switches S3 and S6 are permanently in “ON” state.

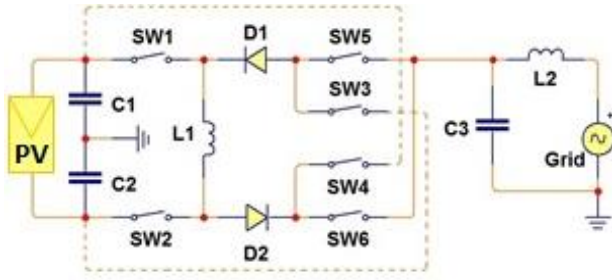


Fig. 2. Modification of the “FIST” topology.

In the buck mode, S2 is in “OFF” state, and S1 operate with Pulse Width Modulation (PWM) frequency. When S1 goes in “ON” state, the current through inductor L1 goes from the positive terminal of the PV through the diode D2, the switch S6 to the grid. When S1 goes open then current flies from the negative terminal via S3, D1, L1, D2, S6.

In the boost mode S1 is permanently “ON”, and S2 operate at PWM frequency. The current through L1 increases and flows through the positive terminal of the PV, S1, L1, S2 to the negative PV-terminal. When S2 is in “OFF” state, the current path is from the positive PV-terminal through S1, L1, D2, S6 to the grid.

In the buck-boost mode, the switches S1 and S2 operate simultaneously. If these switches are in “ON” state, the current through L1 increases. When they are in “OFF” state, the current path is from the negative PV-terminal through S3, D1, L1, D2, S6 to the grid.

All of the above-mentioned switching sequences are controlled by the current half-wave, not by the voltage half-wave. Both half-waves will not coincide if the power factor not equal to one.

The features of this topology define different dependency between input and output voltages. In the paper will be discussed the three modes consistently.

3 Types of modes

3.1. Buck mode

The main equation is that of the balance of the power:

$$0,5U_{PV}I_{10}D - 0,5U_{PV}D'I_0 = u_g I_{20}, \quad (1)$$

$$I_{10} = DI_{20}, \quad (2)$$

where U_{PV} is the full voltage of the photovoltaic, I_{10} , I_{20} are the average values respectively of the currents i_1 and i_2 , D is the duty cycle, $D' = 1 - D$ and u_g is the passing value of the grid voltage.

From equations (1) and (2) follows:

$$u_g = 0,5U_{PV}(D - D') = 0,5U_{PV}(2D - 1). \quad (3)$$

3.2. Boost mode

At this mode during the period DT the inductance L1 will be connected to the full voltage U_{PV} , during the remainder of the period – to its half value.

The equation of the power balance is:

$$DU_{PV}I_{10} + 0,5D'U_{PV}I_{10} = u_g I_{20}, \quad (4)$$

where

$$I_{20} = kD'I_{10}. \quad (5)$$

Here k is the ratio between the average value of i_{10} in the period $(1 - D)T$ and I_{10} :

$$k = \frac{i_{10(1-D)}}{I_{10}}. \quad (6)$$

The value of this coefficient k is close to one, and can be taken as $k \approx 1$.

From (4), (5) and (6) for the grid voltage u_g follows

$$u_g = 0,5U_{PV} \frac{1 + D}{D'}. \quad (7)$$

3.3. Buck-Boost mode

Here the conclusions will be based also on the power balance. A special feature is, that during the period DT is connected the full voltage U_{PV} , during the remainder – its half value with reversed sign.

$$U_{PV}I_{10}DT - 0,5U_{PV}I_{10}D'T = u_g I_{20}T \quad (8)$$

Considering (5) and (6):

$$u_g = 0,5 \frac{3D - 1}{D'}. \quad (9)$$

4 Limits of the proposed topology

Interesting aspect is the value of the power factor, which keeps the topology’s operating ability.

In Fig. 3 is shown the case when the current curve is behind the voltage curve. The values of the voltage in the moments when the current cross the zero line are $+U_0$ and $-U_0$. If absolute values of $|+U_0|$ and $|-U_0|$ are higher than $U_{PV}/2$, during the freewheeling period the subtraction between them will lead to uncontrollable increase of the current and dangerous situation.

The values $+U_0$ and $-U_0$ can be expressed via the angle φ :

$$+U_0 = U_g \sqrt{2} \sin \varphi \quad (10)$$

and

$$-U_0 = U_g \sqrt{2} \sin(\varphi + \pi), \quad (11)$$

where U_g is the effective value of the grid voltage.

Then

$$U_{PV} > U_g \sqrt{2} \sin \varphi = U_g \sqrt{2} \sqrt{1 - \cos^2 \varphi},$$

$$\cos \varphi > \sqrt{1 - \frac{U_{PV}^2}{2U_g^2}} \quad (12)$$

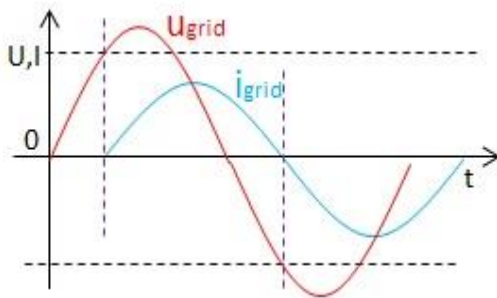


Fig. 3. About the $(\cos \varphi)_{\min}$ calculation.

To avoid a critical value of $\cos \varphi$, it is necessary to introduce a security coefficient k_s , which value will be practically defined in further research. The introduction of this coefficient leads to the following modification of the inequality:

$$\cos \varphi \geq k_s \sqrt{1 - \frac{U_{PV}^2}{2U_g^2}}. \quad (13)$$

5 Simulations and results

In the paper are presented simulations only for a buck-boost mode due to its main advantage that it is the only one, able to work independently. The topology can operate also in buck and boost mode but not independently, only with transition between both modes. That will be object of the future research.

The operation principle of the topology is modelled and simulated via SIMetrix/SIMPLIS Elements© software. The simulation model is shown in Fig. 4.

The photovoltaic is represented by the two sources V1 and V2. Because of the lack of capacitors in the scheme, the middle point between V1 and V2 is grounded. V1 and V2 are ideal sources and that is equivalent of operation with capacitors with infinitely high capacitance. The grid is presented with the source V3 ($U_{\max} = 340$ V), and frequency of 50 Hz. The resistor R1 play role as the resistance of the grid.

The simulation model repeats the topology from Fig. 2, but with ideal switches.

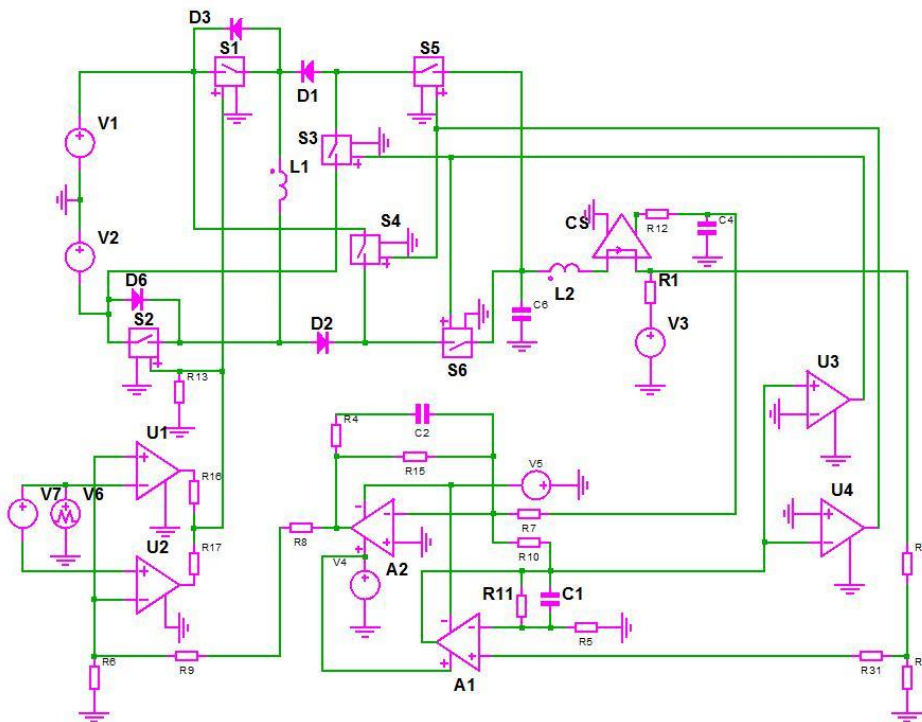


Fig. 4. Simulation model of the proposed topology.

The other components have a control function. Two comparators U3 and U4 change their state with the change of the “set” current direction (output of the amplifier A1) and control the switches S3, S4, S5 and S6. The comparators U1 and U2 control the switches S1 and S2. Their control inputs are connected together, so they operate simultaneously, which creates the buck-boost mode. The outputs of comparators U1 are connected via equal resistors R2 and R3 with the control inputs of the switches S1 and S2, so each comparator can control them. To the inputs of the mentioned comparators are applied voltages with triangle to sawtooth form, called in this paper as “TS” form. These TS voltages are generated from the source V6, in concrete case with a frequency 50 Hz. This positive voltage is transferred by the DC source V7 to the negative area. The values of voltages of V6 and V7 are equal and that way are formed two TS voltage carriers.

To the other inputs of V6 and V7 is applied the control voltage $U_{Control}$. The pulses are formed in the crossing points of $U_{Control}$ and the TS voltages. The $U_{Control}$ voltage is generated from the operational amplifier A2. It has a frequency-dependent feedback, which gives a proportional - integral behaviour. On the input of A2 are applied signal from the current sensor CS and a “set” signal for the current.

This signal must have a sinusoidal form and must be shifted toward the grid voltage at an exact angle. There are many possibilities to become such displaced signal (this is not an aim of this paper). In the presented model this shifted signal comes from the output of the amplifier A1 due to a frequency dependent negative feedback formed from the elements R11 and C1. The same signal is used to control of the comparators U3 and U4, because it controls the direction of the current.

The operation of the comparators U1 and U2 and the switches S1 and S2 is illustrated in Fig. 5. The TS carrier “a” is generated from the source V6. The TS carrier “b” is shifted in the negative area via the DC source V7. Both TS voltages touch the zero line.

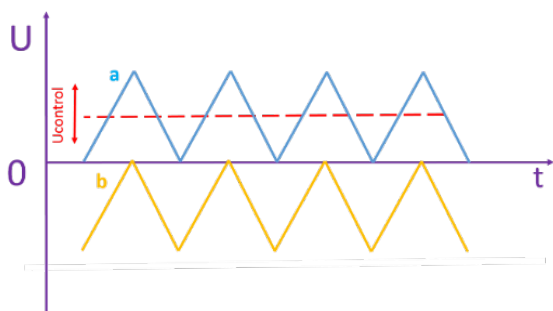


Fig. 5. Position of the carriers “a” and “b” and the control voltage.

The control voltage $U_{Control}$ can vary and change its position in the positive and the negative areas. The pulses are formed from the crossing points between the control voltage $U_{Control}$ and the respective TS line. Therefore, in zero position of $U_{Control}$, the pulse width

will be zero. At shift in both directions, the pulse width increases.

The result from the simulation is shown in Fig. 6. The green line is the injected current and the red line is the voltage of the grid. The current lags behind the voltage in this case but with small changes in the schematic, the voltage line can go to the right of the current line.

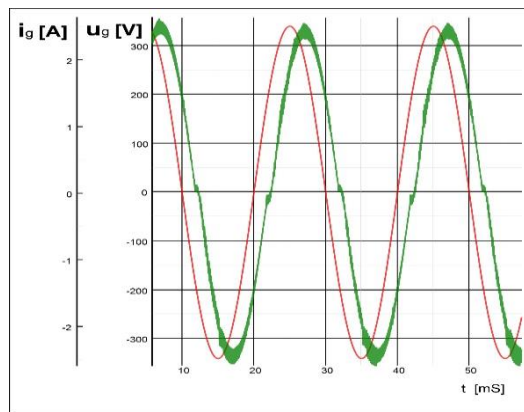


Fig. 6. Grid voltage and injected grid current.

It is evident that the curves shown good sinusoidal form with minimum disturbance regardless of the angle of the phase with the voltage sinusoid.

6 Conclusions

In this article is proposed a topology of an inverter, transformerless connected to a single-phase grid, which can work with variable power factor, thus compensate the reactive power of consumers in the proximity of the renewable source (photovoltaic or other). The presented topology is a modified design of a topology with flying inductor and symmetric circuit for both half-waves, which operates only with power factor, equal to one.

Advantage of this topology with flying inductor is that there is no need from a separate boost inverter.

As an advantage of the proposed topology may be specified that it allows of the power factor to vary from one to a limit, depend of the input voltage. This variation is attained through a shift of the “set” current toward the grid voltage. The proposed topology can also perform inverting of both active and reactive power in the electrical grid.

Because of its symmetry, the topology can be easily controlled by fairly simple scheme. Other positive feature of the symmetric circuit is the easily prevention of DC component in the injected current.

Similarly to the unmodified topology, the modified can also operate in all modes in both half-waves of the current. So it gives wide application for different powers and voltages of the PV-plants. In the current article is observed only the operation in buck-boost mode.

The question with the variable power factor is of interest, the change can be controlled automatically by

the real reactive power consumption. This is not an aim of this paper, can be of other work.

This work has been supported by the National Scientific Program "Young scientists and postdoctoral researchers", which is gratefully acknowledged by the authors.

References

1. L. Hassine, E. Olias, J. Quintero, M. Haddadi, Digital power factor control and reactive power regulation for grid-connected photovoltaic inverter, *Renewable Energy*, **34**, 315-321, (2009).
2. E. Demirok, P. Gonzalez, K. Frederiksen, D. Sera, P. Rodrigues, R. Teodorescu, Local reactive power control methods for overvoltage prevention of distributed solar inverters in low-voltage grids, *IEEE Journal of Photovoltaics*, **1**, 174-182, (2011).
3. S. Huang, F. Pai, Design and operation of grid-connected photovoltaic system with power-factor control and active islanding detection, *IEEE Proc. Transm. Distrib.*, **148**, 243-250, (2001).
4. T. Wu, H. Nien, C. Shen, T. Chen, A single-phase inverter system for PV power injection and active power filtering with nonlinear inductor consideration, *IEEE Transactions of Industry Applications*, **4**, 1075-1083, (2005).
5. Yu-Kang Lo, Jin-Yuan, Tin-Yuan Wu, Grid-Connection Technique for a Photovoltaic System with Power Factor Correction" IEEE PEDS, 522-525 (2005).
6. T.-F. Wu, C.-H. Chang, Y.-K. Chen, A Multi-Function Photovoltaic Power system with Grid-Connection and Power Factor Correction Features, *Proc IEEE 31st Annual Power Electronics Specialists Conference*, 1185-1190, (2000).
7. S. Kim, Gwonjong Yoo, J. Song, A bifunctional utility connected photovoltaic system with power factor correction and UPS facility, *Proc. Photovoltaic Specialists Conference IEEE*, 1363-1368, (1996).
8. T. Kerekes, R. Teodorescu, M. Liserre. Common Mode Voltage in Case of Transformerless PV Inverters Connected to the Grid. *Proc. of the 2008 IEEE International Symposium on Industrial Electronics*, 2390-2395, (2008)
9. N. Lokhande, G. Phadnis. Comparison of full bridge transformerless H5, HERIC, H6 inverter topologies. *International Journal of Innovative Research in Science, Engineering and Technology*, **6**, 10870-10881, (2017).
10. A. Mirev, A. Andonov, Y. Rakanov. Photovoltaic's inverter directly connected to the grid. *Science, Engineering & Education*, **1**, 32-35, (2016).
11. Y. Rakanov, A. Mirev, J. Javorova, A. Andonov, Transformerless Grid Connected Inverter for Photovoltaics. *Proc. of the Intern Conf "Alternative Energy Sources, Materials & Technologies AESMT'19"*, Sofia, (2019) (under print).
12. N. Kasa, T. Iida. Flyback Type Inverter for Small Scale Photovoltaic Power System. *Proc. of IEEE 28th Annual Conf of the Industrial Electronics Society*, **2**, 1089-1094 (2002).
13. E. Gubia, P. Sanchis, A. Ursua. Ground currents in single-phase transformerless photovoltaic systems. *Progress in Photovoltaics: Research and Applications*, **15**, 629-650, (2007).
14. N. Kasa, T. Iida, H. Iwamoto. An Inverter Using Buck-boost Type Chopper Circuits for Popular Small-scale Photovoltaic Power System. *Proc. of the 25th Annual Conference of the IEEE Industrial Electronics Society*, **1**, 185-190, (1999).
15. N. Kasa, H. Ogawa, T. Iida, H. Iwamoto. A Transformerless Inverter Using Buck-boost Type Chopper Circuit for Photovoltaic Power System. *Proc. of the IEEE 1999 International Conference on Power Electronics and Drive Systems, Hong Kong*, 653-658, (1999).